Agricultural and Forest Meteorology 252 (2018) 269–282

Contents lists available at ScienceDirect

Agricultural and Forest Meteorology

journal homepage: www.elsevier.com/locate/agrformet

Warmer temperatures reduce net carbon uptake, but do not affect water use, in a mature southern Appalachian forest

A. Christopher Oishi[a,*], Chelcy F. Miniat[a], Kimberly A. Novick[b], Steven T. Brantley[c], James M. Vose[d], John T. Walker[e]

[a] USDA Forest Service, Southern Research Station, Coweeta Hydrologic Laboratory, 3160 Coweeta Lab Road, Otto, NC 28763, USA
[b] School of Public and Environmental Affairs, Indiana University – Bloomington, 702 N. Walnut Grove Avenue, Bloomington, IN 47405, USA
[c] Joseph W. Jones Ecological Research Center, 3988 Jones Center Drive, Newton, GA 39870, USA
[d] USDA Forest Service, Southern Research Station, Center for Integrated Forest Science, 5223 Jordan Hall, Box 8008, College of Natural Resources, Forestry and Environmental Resources, North Carolina State University, Raleigh, NC 27695, USA
[e] U.S. Environmental Protection Agency, Office of Research and Development, 109 T.W. Alexander Dr., Durham, NC 27711, USA

ARTICLE INFO

Keywords:
Net ecosystem exchange
Net ecosystem productivity
Complex terrain
Drought
Gross primary productivity
Ecosystem respiration

ABSTRACT

Increasing air temperature is expected to extend growing season length in temperate, broadleaf forests, leading to potential increases in evapotranspiration and net carbon uptake. However, other key processes affecting water and carbon cycles are also highly temperature-dependent. Warmer temperatures may result in higher ecosystem carbon loss through respiration and higher potential evapotranspiration through increased atmospheric demand for water. Thus, the net effects of a warming planet are uncertain and highly dependent on local climate and vegetation. We analyzed five years of data from the Coweeta eddy covariance tower in the southern Appalachian Mountains of western North Carolina, USA, a highly productive region that has historically been under-represented in flux observation networks. We examined how leaf phenology and climate affect water and carbon cycling in a mature forest in one of the wettest biomes in North America. Warm temperatures in early 2012 caused leaf-out to occur two weeks earlier than in cooler years and led to higher seasonal carbon uptake. However, these warmer temperatures also drove higher winter ecosystem respiration, offsetting much of the springtime carbon gain. Interannual variability in net carbon uptake was high (147 to 364 $g\,C\,m^{-2}\,y^{-1}$), but unrelated to growing season length. Instead, years with warmer growing seasons had 10% higher respiration and sequestered ~40% less carbon than cooler years. In contrast, annual evapotranspiration was relatively consistent among years (coefficient of variation = 4%) despite large differences in precipitation (17%, range = 800 mm). Transpiration by the evergreen understory likely helped to compensate for phenologically-driven differences in canopy transpiration. The increasing frequency of high summer temperatures is expected to have a greater effect on respiration than growing season length, reducing forest carbon storage.

1. Introduction

Increasing air temperature (T_{air}) is a highly ubiquitous and influential climate driver affecting terrestrial ecosystems, with the potential to alter key ecosystem services such as carbon sequestration and water yield. Warmer temperatures can advance the date of leaf-out and delay the date of leaf senescence in a variety of ecosystems, particularly temperate, boreal, and subalpine forests, increasing the number of days for plants to assimilate carbon (C) and transpire water (Richardson et al., 2013). However, warmer temperatures will also affect ecosystem processes throughout the year, with potentially positive or negative impacts on C and water dynamics. Higher T_{air} leads to an increase in potential evapotranspiration linked to rising atmospheric demand for water (vapor pressure deficit; *D*), which could result in reduced water yield (Creed et al., 2014). However, actual evapotranspiration (ET) and photosynthesis may be constrained by reduced stomatal conductance at high *D* (Novick et al., 2016a) and non-stomatal temperature limitations to photosynthesis (Zhou et al. 2014). Although photosynthesis represents the gross input of C to the ecosystem, the net ecosystem C balance depends on the difference between photosynthesis and respiration, both of which may be enhanced with warmer temperatures (Baldocchi et al., 2017; Davidson and Janssens, 2006)). During comparatively warmer seasons, the magnitude of increased ecosystem photosynthesis tends to exceed the increase in respiration during the

* Corresponding author.
E-mail address: acoishi@fs.fed.us (A.C. Oishi).

https://doi.org/10.1016/j.agrformet.2018.01.011
Received 28 August 2017; Received in revised form 3 January 2018; Accepted 5 January 2018
0168-1923/ Published by Elsevier B.V.

Table 1
Species list, basal area, and maximum leaf area index, based on allometric equations from four 25 × 25 m plots near the base of the eddy covariance tower, sorted by leaf area index (see Methods).

Scientific name	Common name	Basal area		Leaf area index	
		($m^2\ ha^{-1}$)		($m^2\ m^{-2}$)	
Betula lenta L.	Black (sweet) birch	3.19	10.9%	1.05	22.6%
Liriodedron tulipifera L.	Tulip (yellow) poplar	6.94	23.8%	0.81	17.5%
Quercus alba L.	White oak	5.09	17.5%	0.65	14.0%
Rhododendron maximum L.	Great (rosebay) rhododendron	4.39	15.1%	0.60	12.9%
Acer rubrum L.	Red maple	2.18	7.5%	0.44	9.5%
Nyssa sylvatica Marsh.	Blackgum	2.06	7.1%	0.33	7.1%
Oxydendrum arboreum L. (DC.)	Sourwood	1.89	6.5%	0.27	5.8%
Carya spp.	Hickory species	0.80	2.7%	0.13	2.8%
Fagus grandifolia Ehrh.	American beech	0.62	2.1%	0.10	2.2%
Quercus velutina Lam.	Black oak	0.46	1.6%	0.08	1.7%
Cornus florida L.	Flowering dogwood	0.32	1.1%	0.05	1.1%
Kalmia latifolia L.	Mountain laurel	0.25	0.9%	0.04	0.9%
Carpinus caroliniana Walter	American hornbeam	0.19	0.7%	0.03	0.6%
Quercus rubra L.	Red oak	0.17	0.6%	0.02	0.4%
Fraxinus americana L.	White ash	0.14	0.5%	0.02	0.4%
Tsuga canadensis L.	Eastern hemlock	0.31	1.1%	0.01	0.2%
Pinus strobus L.	Eastern white pine	0.08	0.3%	0.01	0.2%
Magnolia fraseri Walter	Mountain (Fraser) magnolia	0.05	0.2%	< 0.01	< 0.2%
Ilex opaca Aiton	American holly	0.02	0.1%	< 0.01	< 0.2%
TOTAL		29.14		4.64	

spring (Richardson et al., 2010), but increases in respiration may exceed the increase in photosynthesis in the fall (Piao et al., 2008). Thus, through respiration, global trends in temperature can have a large influence on ecosystem C balance (Ballantyne et al., 2017).

Maintaining high primary productivity and water use throughout the growing season requires favorable climatic conditions beyond just temperature. Without an adequate water supply, an earlier start to the growing season has the potential to lead to a more rapid depletion of soil water, limiting both photosynthesis and transpiration later in the growing season (Williams et al., 2013), offsetting any gains from earlier leaf-out (Wolf et al., 2016). However, soil respiration may be suppressed during dry periods (Davidson et al., 1998) resulting in lower annual soil and ecosystem respiration during warm, drought years compared to more mild years (Novick et al., 2015; Palmroth et al., 2005). At the other end of the spectrum, periods of high precipitation (*P*) are often characterized by cloudy days, where radiation may limit photosynthesis and high humidity may limit ET. Therefore, the magnitude and timing of precipitation, particularly during the growing season, also affects C and water dynamics.

The dynamics governing precipitation and temperature impacts on primary productivity and water use are particularly important in areas of complex terrain, where orographic rainfall patterns can lead to exceptionally high water inputs, and where topographic complexity can result in large spatial variability in microclimate (Daly et al., 2017; Burt et al., 2017). Coves and valleys can benefit from a downslope subsidy of soil water (i.e. water drainage from upslope area), reducing the impacts of lower precipitation on transpiration, conductance (Hawthorne and Miniat 2017) and productivity (Elliott et al., 2015a, Elliott et al., 2015a, b). Furthermore, nocturnal cold air drainage into low-lying valleys can suppress respiration, enhancing the C sink (Novick et al., 2016b) and isolating down-slope positions from macro-scale climate variability. Therefore, topographic complexity may help to buffer the local microclimate from regional climate change (McLaughlin et al., 2017). These montane ecosystems can therefore play an important role in sequestering C and regulating water yield, but due largely to methodological challenges (Novick et al. 2014), have been historically underrepresented in flux observation networks and thus may not be accurately characterized by global models.

Our goal was to examine the long- and short-term climate drivers of carbon gain and water loss in a southern Appalachian deciduous forest located in a low-elevation, cove position. These forests have high diversity of overstory tree species, exhibiting isohydric and anisohydric hydraulic strategies, and dense understory vegetation with a significant evergreen shrub component. The southern Appalachian region of the southeastern United States is an extensively forested area, characterized by complex topography and large amounts of annual rainfall, often exceeding 2 m of rain per year. This region's mesic, temperate climate has high potential for carbon gain and provides a critical source of drinking water to major cities in the southern US (Caldwell et al., 2016). T_{air} in this region has been increasing since the early 1980s at approximately 0.5 °C per decade (Ford et al., 2011). This trend is affecting both dormant and growing season temperatures. Warmer temperatures in these forests are expected to lead to an earlier start and later end to growing seasons and subsequently greater ET (Hwang et al., 2014). Mean precipitation has not shown a temporal trend at the annual scale, in part due to decreases in July compensated by increases in late fall, but variability in mean annual precipitation is increasing (Ford et al., 2011).

We analyzed five years of eddy covariance data (2011–2015) from Coweeta Hydrologic Laboratory in western North Carolina, United States. Leaf phenology was used to estimate growing season length. To address methodological challenges associated with using eddy covariance techniques in complex terrain (Novick et al., 2013), we incorporated forest water yield data from gauged watersheds and shorter-duration measurements of subcanopy eddy covariance and soil CO_2 efflux, to examine seasonal and interannual ecosystem exchange of carbon and water. Using these multiple data sets, we explored the relative importance of growing season length versus intra-annual variability in climate as drivers of annual ET and net C uptake. Finally, we leveraged eight decades of local climate records to assess the impact of long-term trends in climate on forest water yield and C storage in a relatively understudied biome.

2. Materials and methods

2.1. Site description

The forest surrounding the Coweeta flux tower (35.059N, 83.427W, 690 m asl) was selectively harvested in the 1930s and has naturally regenerated since then. Tree surveys were conducted in four, 25 by 25 m plots near the base of the tower. All trees with diameter at breast height (DBH, cm) greater than 10 cm were tagged and re-measured

annually. Canopy height was ~35 m and stem density was 404 trees > 10 cm DBH per hectare. The forest canopy was dominated by tulip poplar, red maple, black birch, white oak, and hickories (Table 1). Eastern white pine was present, but rare (~8 trees ha^{-1}). The evergreen shrub, rosebay rhododendron (*Rhododendron maximum* L.) occurred in dense thickets and reached over 4 m in height in many cases. Canopy leaf area index (L, m^2 leaf area m^{-2} ground area) was estimated using species-specific allometric relationships based on DBH generated from data collected at Coweeta (Martin et al., 1998).

2.2. Leaf phenology

Leaf phenology was monitored by ground-based, optical measurements (LAI-2000, LI-COR, Lincoln, NE) ranging from monthly to bi-weekly during 2011–2013. Leaf phenology was also estimated using, a digital camera (NetCam SC, StarDot Technologies, Buena Park, CA) from the PhenoCam Dataset (V1.0; Richardson et al., 2017) installed on the tower in April, 2011. Sigmoidal curves were fitted to time series of the daily greenness chromatic coordinate (GCC, ratio of green color channel to sum of red, green, and blue color channels; Sonnentag et al., 2012) measurements for the spring and fall periods of each year (SigmaPlot 13.0, Systat Software Inc., San Jose, CA). Dates when canopy leaf area expansion and senescence reached 25%, 50%, and 75% of maximum (L_{25}, L_{50}, L_{75}, respectively) were estimated from these curves. Estimated leaf expansion trends were well-correlated with the ground-based optical measurements (LAI-2000, LI-COR, Lincoln, NE), ranging from monthly to bi-weekly during 2011–2013, based on seasonal polynomial functions and were used to estimate time series of expansion of canopy L (See Supplementary A.2 for details).

2.3. Eddy covariance and micrometeorology

Ecosystem fluxes of carbon dioxide (as net ecosystem exchange; NEE, $g\,C\,m^{-2}\,s^{-1}$) and water vapor (as latent heat flux, converted to ET) were estimated using an eddy covariance system installed on a 37-m walk-up tower. Equipment and data processing methods were previously described in Novick et al. (2013) and are summarized in the Supplementary A.2. Briefly, the system comprised a closed path infrared gas analyzer (EC155, Campbell Scientific, Logan, UT) and sonic anemometer (Model 81000, R.M. Young Company, Traverse City, MI). Raw 10-Hz data were processed into hourly averages. Storage fluxes were estimated using an atmospheric profile system (prototype AP200, Campbell Scientific), consisting of a closed-path infrared gas analyzer (LI-840; LI-COR, Lincoln, NE, USA) connected to air intake ports with co-located sonic anemometers at heights of 4, 9, 16, 24, 30, and 37 m. Latent heat flux data were gapfilled using the marginal distribution method (Reichstein et al., 2005; Novick et al., 2009). Net ecosystem exchange data were gapfilled using the "Online eddy covariance gapfilling and flux partitioning tool" (http://www.bgc-jena.mpg.de/~MDIwork/eddyproc/index.php).

Carbon and water fluxes from the soil and herbaceous vegetation were estimated using a subcanopy eddy covariance system, located approximately 35 m southwest of the tower. The subcanopy system comprised an open path infrared gas analyzer (LI-7500, LI-COR, Lincoln, NE), sonic anemometer (Model 81000, R.M. Young Company, Traverse City, MI), and a net radiometer (NR-Lite, Kipp & Zonen, Delft, The Netherlands), all installed at approximately 2 m above the forest floor. Data from this system were analyzed for 2013–2015 and processing was similar to the canopy system; however, given the slope at the base of the subcanopy system, a correction for wind angle was added.

Air temperature ($T_{air,}$ °C) and relative humidity were measured at 2/3 canopy height (HMP-45, Vaisala, Helsinki, Finland) and used to estimate vapor pressure deficit (D, kPa). Photosynthetically active radiation (PAR; LI-190, LI-COR Biosciences, Lincoln, NE) and upward and downward, shortwave and longwave radiation (CNR 4, Kipp & Zonen, Delft, The Netherlands) were measured above the canopy at 37 m. Volumetric water content (VWC) was estimated as the average of eight arrays of soil moisture measurements, each consisting of four time domain reflectometry probes (CS615 and CS616, Campbell Scientific), installed horizontally at 5, 20, and 35 cm depths, and one vertically at 65–95 cm depth.

2.4. Precipitation interception

Precipitation volume (P, ml) reaching the forest floor as throughfall (P_T, mm) was collected using twelve throughfall collectors, each consisting of a 20 cm diameter funnel connected to a five-gallon bucket. Throughfall volume measurements were made monthly in the field with a graduated cylinder, and converted to depth. We estimated throughfall on a storm event basis using the following equation:

$$P_T = a \times P + b \times P_n \quad (1)$$

where a and b are fitted parameters, P is recorded at a proximate, open field climate station approximately 275 m from the tower, and P_n is the number of precipitation events within a collection period (separate precipitation events were defined by a dry period of at least four-hours). Approximately half of the collection periods had four or fewer rain events and collection periods with a greater number of events became increasingly infrequent. Therefore, to avoid overweighting the rare collection periods with many rain events, data were restricted to collections with fewer than five events. Thus, for a single precipitation event, the b parameter represents the intercept or the minimum threshold of P to result in P_T, and the a parameter is the slope, or the proportion of subsequent precipitation to reach the forest floor. Hourly P_T was then estimated by first identifying individual precipitation events, then for the first b mm of precipitation each event, P_T was zero, and finally, any subsequent P resulted as $P_T = a \times P$.

Precipitation intercepted by the canopy was estimated as the difference between P and P_T. However, since intercepted P is not immediately evaporated and evaporated interception (E_I, mm) is often under estimated using eddy covariance methods, we partitioned E_I using the following approach. We positioned three leaf wetness sensors (model 237-L, Campbell Scientific, Logan, UT) on the tower for spring and summer of 2016, day of year (DOY) 44-215, and determined the length of time after a precipitation event for them to dry. We then partitioned half of accumulated intercepted precipitation to be evaporated at each hourly time step (with a maximum rate of $1\,mm\,h^{-1}$) during daytime hours. Canopy ET was estimated as E_I when E_I exceeded tower-based ET.

2.5. Soil CO_2 efflux and ecosystem respiration

We used two independent approaches for estimating soil CO_2 efflux (F_{soil}, μ mol $CO_2\,m^{-2}$ ground area s^{-1}). The first approach was designed to capture spatial variability of F_{soil} using a portable soil CO_2 system (LI-6400, LI-COR, Lincoln, NE) along two 350 m long transects extending from the tower within the primary footprint of daytime fluxes (Novick et al., 2014). Along each transect, 13 measurement points were established at 25 m spacing by installing plastic collars to 5 cm depth in the mineral soil. Measurements were made approximately weekly from July 23 to November 15, 2013 and May 21 to August 6, 2014.

The second approach was optimized to capture temporal variability of F_{soil} using an automated system comprised of 15 sequentially sampled soil chambers (Automated CO_2 Efflux System; USDA Forest Service, US Patent 6,692,970) located approximately 50 m southwest of the tower and 15 m from the subcanopy eddy covariance system. Data were processed and used to establish daily mean fluxes for each chamber based on Oishi et al. (2013). This system was in operation from August 18, 2013 through December 30, 2014. The close proximity of the automated F_{soil} and subcanopy eddy covariance systems also

Table 2
Monthly, seasonal*, and annual mean air temperature (T_{air}) over the five-year study period and using the 80-year long-term data from Coweeta Climate Station 01. Bold numbers indicate monthly or seasonal maxima, italicized numbers indicate monthly or seasonal minima.

	2011	2012	2013	2014	2015	5-year mean (SD)	80-year mean (SD)
January	1.0	4.7	**6.6**	*−0.6*	3.4	3.0 (2.9)	3.5 (2.7)
February	**6.2**	6.3	4.1	5.4	*1.3*	4.7 (2.1)	4.8 (2.2)
March	10.1	**13.3**	*5.5*	8.2	10.8	9.6 (2.9)	8.5 (2.1)
April	**14.9**	14.8	*13.6*	13.9	14.8	14.4 (0.6)	12.9 (1.4)
May	17.4	**19.1**	*16.7*	17.7	18.9	18.0 (1.0)	16.7 (1.1)
June	**21.9**	*20.7*	21.5	21.8	22.3	21.6 (0.6)	20.3 (1.0)
July	24.0	**24.2**	22.4	*21.6*	23.3	23.1 (1.1)	22.0 (1.0)
August	**22.9**	*21.7*	21.9	22.0	22.3	22.2 (0.4)	21.6 (1.0)
September	*18.7*	19.1	19.4	**21.2**	19.7	19.6 (1.0)	18.6 (1.1)
October	*12.1*	13.4	13.9	14.2	**14.4**	13.6 (0.9)	13.3 (1.4)
November	8.6	7.5	6.9	*6.2*	**10.8**	8.0 (1.8)	8.2 (1.6)
December	*5.7*	6.9	6.4	7.6	**10.4**	7.4 (1.8)	4.5 (2.2)
JFMA	8.0	**9.8**	7.5	*6.7*	7.7	7.9 (1.2)	7.4 (1.2)
MJJA	**21.6**	21.4	*20.6*	20.8	21.7	21.2 (0.5)	20.2 (0.8)
SOND	11.3	11.7	*11.6*	12.3	**13.8**	12.1 (1.0)	11.1 (1.0)
Annual	13.7	14.4	*13.3*	*13.3*	**14.5**	13.8 (0.6)	13.0 (0.7)

*Seasonal averages are grouped in four-month periods: January–April (JFMA), May–August (MJJA), and September–December (SOND).

allowed us to compare these two approaches for estimating soil carbon fluxes.

Temperature sensitivity parameters for F_{soil} were fitted for both methods and each measurement location to an exponential equation using the *nlinfit* function in MATLAB (Mathworks, Natick, MA):

$$F_{soil} = a \times \exp(b \times T_{soil}), \quad (2)$$

where the a parameter represents the base respiration at 0 °C (μ mol CO_2 m^{-2} ground area s^{-1}) and the b parameter represents temperature sensitivity. From these estimates, we calculated Q_{10}, representing the factorial change in F_{soil} to a 10 °C increase in T_{soil}:

$$Q_{10} = \exp(10 \times b). \quad (3)$$

Leaf respiration (R_{leaf}, μmol CO_2 m^{-2} leaf area s^{-1}) was estimated using an exponential temperature-response function based on species-specific parameters from previous work performed near this site (Bolstad et al., 1999):

$$R_{leaf} = R_{Tref} \times Q_{10}^{(T_{air}-T_{ref})/10} \quad (4)$$

where T_{ref} is a reference temperature (10 °C), R_{Tref} is a species-specific respiration rate at T_{ref} (μmol CO_2 m^{-2} leaf area s^{-1}) and Q_{10} is a species-specific sensitivity parameter and T_{air} is hourly nighttime data. R_{leaf} was scaled to the stand level based on estimated L for each species (Table 1) and the annual time series of L. Total ecosystem respiration (R_E, g C m^{-2} s^{-1}) was estimated as the sum of R_{leaf} and F_{soil}. For comparison, we also estimated R_E by fitting the relationship of T_{soil} and nighttime NEE to an exponential function (assuming that photosynthesis is zero at night and NEE = R_E) and extrapolating daytime fluxes (Dragoni et al., 2011). Gross ecosystem productivity (GEP, g C m^{-2} s^{-1}) was estimated as NEE– R_E.

2.6. Photosynthetic phenology

Phases of the growing season were also estimated based on eddy covariance carbon fluxes following Gu et al. (2003). In this approach, five-parameter Weibull curves were fitted to maximum daily GEP data for the first half and second half of each year, establishing time series of potential photosynthetic capacity of the ecosystem (GEP_{max}; μ mol CO_2 m^{-2} s^{-1}). The resulting and the inflection points of each curve were used to characterize the timing and rate of change in photosynthetic activity in the spring and fall. (See Supplementary A.5 for details).

2.7. Long-term site data

Air temperature, relative humidity, and precipitation have been measured near the eddy covariance tower at Coweeta climate station 01 since 1936 (Laseter et al., 2012). The long-term T_{air} record consists of daily maximum and minimum recorded on a standard max-min thermometer. Daily mean T_{air} was estimated as the average of these two values. Total solar radiation (W m^{-2}) has been measured since 1960 and mean daily radiation from the climate station was well correlated with downwelling shortwave radiation data from the tower (r^2 = 0.99). Runoff (Q, mm) estimated from weirs at the base of watersheds (watersheds #2, 14, and 18; (Caldwell et al., 2016) with similar stand age and aspect was combined with precipitation data as an independent estimate of ET (ET = $P - Q$).

2.8. Statistical analyses

Correlation analysis was used to test whether growing season length increased with T_{air}. Specifically, dates of spring L_{50} were correlated with heating degree days greater than 0 °C (HDD_0, the cumulative number of degrees daily mean temperature is above 0 °C). We tested combinations of consecutive days ranging from January 1 through April 30 (DOY 120) and identified the range of dates with the maximum r^2. Similarly, leaf senescence L_{50} was correlated with cooling degree days less than 20 °C (CDD_{20}) between DOY 210 and 290 (range based on (Hwang et al., 2014)). Data were fitted to exponential, sigmoidal, and Weibull functions using the nlinfit function in MATLAB. We tested long-term data first for significant piecewise linear regressions, then for significant linear regressions using SigmaPlot (Version 13.0, Systat Software Inc., San Jose, CA). Linear regressions were performed using either MATLAB or SigmaPlot. We also performed a wavelet analysis as an alternative method for identifying the key biophysical drivers of temporal variability in NEE and ET (Supplementary A.6).

3. Results

3.1. Meteorological conditions

The five-year study period included the 1st and 3rd hottest in Coweeta's 80-year long-term record (2015 and 2012, respectively; Table 2). Mean annual T_{air} was above the long-term average for the entire study period (13.0 °C; Table 2). The highest seasonal (four-month) T_{air} values of the study period were observed in the spring of 2012, the summer of 2011, and the fall of 2015 (Fig. 1, Table 2). Years 2013 and 2014 were mild, by comparison. The lowest seasonal T_{air} values of the study period occurred in either of these two years. Although 2012 had the lowest June and August temperatures of the study period, it also had the warmest May and July, resulting in summer and annual temperatures above the five-year average. Monthly temperatures in 2015 dropped below the five-year average only in February and high temperatures in late fall resulted in the highest mean annual temperature.

Annual precipitation ranged from slightly below average in 2014 (within one standard deviation of the long-term mean) to the wettest year on record in 2013 (Fig. 1, Table 2). Despite above average annual P, 2011 experienced the lowest soil moisture (expressed as volumetric water content, VWC; m^3 m^{-3}) of the study period late in the growing season (Fig. 1). In contrast, despite the lowest annual P in 2014, the even temporal distribution maintained moderately high soil moisture throughout the year. High intra-annual variability in P led to moderately dry soil conditions (VWC ~0.25 m^3 m^{-3}), during the early, middle, and late portions of the growing season in 2012, 2015, and 2013, respectively.

The combination of warm, dry conditions in 2011 resulted in

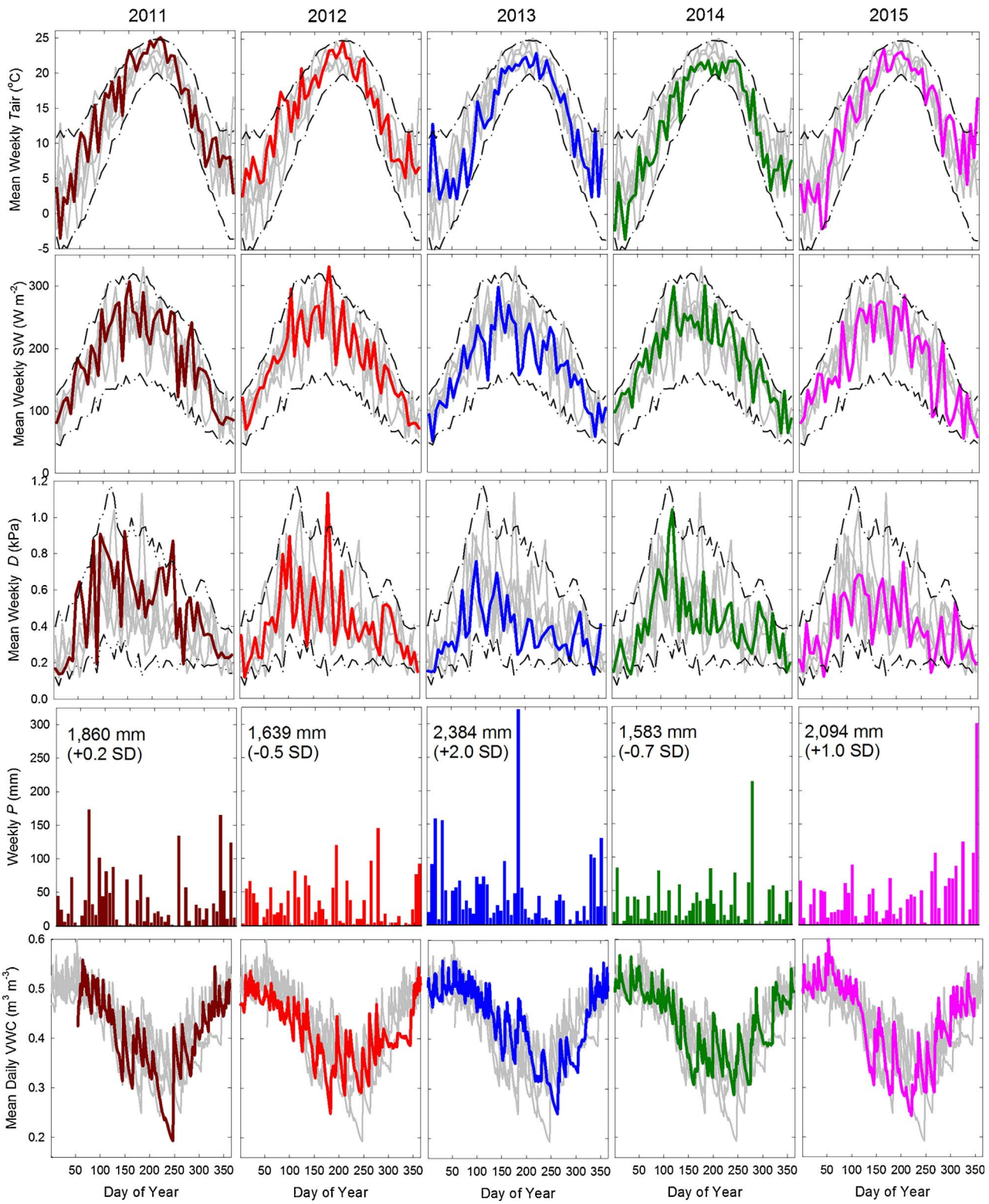

Fig. 1. Mean weekly air temperature (T_{air}), downwelling shortwave radiation (SW), vapor pressure deficit (D) (data represent weekly averages of daily means), total weekly precipitation (P), and daily volumetric soil water content (VWC). Colored lines represent individual years of the current study, gray lines represent data from the other four years of this study (not included for P), dashed lines represent $+/-2$ standard deviations from the long-term mean (1936–2015). Text associated with P indicates total annual P and number of standard deviations (SD) away from long-term mean (1,800 mm, SD = 298 mm).

significantly higher mean daily D for the main portion of the growing season (June–August) compared to other years (0.62 kPa; t-test, $p < 0.003$). In contrast, the rainy, relatively cool growing season in 2013 had a significantly lower mean daily D (0.38 kPa; $p < 0.0001$), whereas all other years were similar (0.49 kPa; $p > 0.08$).

3.2. Leaf phenology

Years with warmer early-spring temperatures resulted in earlier leaf expansion. Leaf expansion occurred earliest in 2012, followed by 2011, then all other years (Fig. 2a). The date at which springtime canopy leaf

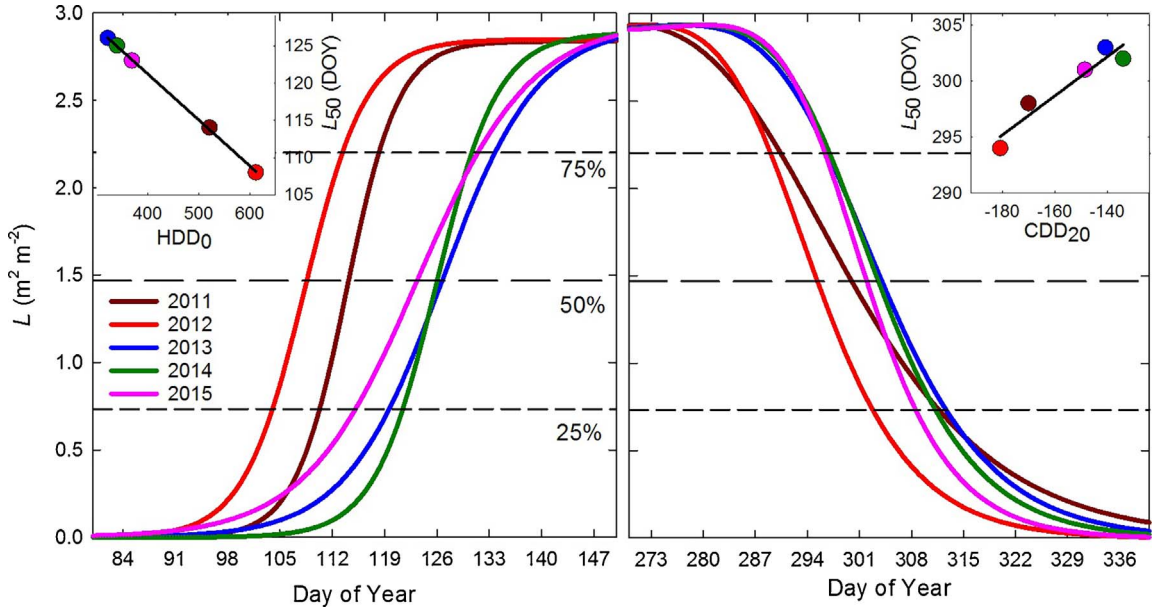

Fig. 2. Seasonal time series of estimated (a) spring and (b) fall canopy leaf area index (L). Dashed horizontal lines represent 25%, 50%, and 75% of maximum canopy leaf area (L_{25}, L_{50}, and L_{75}, respectively). Inset in (a) shows relationship between date of year (DOY) of spring L_{50} and cumulative heating degree days > 0 °C (HDD_0) between day of year 17–83 ($y = -0.0619x + 146.0$; $r^2 = 0.99$; $p < 0.0001$) and (b) shows relationship between DOY of fall L_{50} and cooling degree days < 20 °C (CDD_{20}) between day of year 210–290 ($y = 0.1754x = 326.7$; $r^2 = 0.91$; $p < 0.01$).

area reached 50% of maximum (L_{50}) was nearly two weeks earlier in 2012 than the three cooler years (Table 4). Springtime date of L_{50} was strongly correlated with HDD_0 in February and March ($r^2 = 0.96$; $p < 0.0001$) and produced the best fit using HDD_0 between days of year (DOY) 17–83 ($r^2 = 0.99$; $p < 0.0001$; Fig. 2a).

Years with warmer early-spring temperatures also displayed earlier leaf senescence, which was largely explained by CDD_{20} from DOY 210–290 (Fig. 2b, Table 4). The residual variability did not show any clear relationship with either the timing or magnitude of low soil moisture. Initiation of leaf senescence in 2011 was similar to 2012, but 2011 experienced a slower rate of leaf loss. The variability among years in leaf senescence dates was about half that of leaf expansion dates—within nine days for fall dates of L_{50} compared to within 18 days for spring dates of L_{50} (Table 4).

Although years with warmer early-spring temperatures resulted in both an earlier leaf expansion and senescence, growing season length was longer in warmer years. Growing season length, characterized by the number of days > L_{50} differed by a maximum of nine days among years (Table 4) and showed strong correlation with average T_{air} from DOY 1–90 ($r^2 = 0.92$, $p = 0.01$).

3.3. Ecosystem evapotranspiration

Annual ET showed little interannual variability (Table 3,) and was not related to growing season length, beginning of growing season, or end of growing season ($p > 0.18$ for all leaf expansion levels in Table 4). The years with the highest and lowest annual ET (2012 and 2011, respectively) both had earlier starts, earlier ends, and longer growing seasons than the other years of the study. Leaf expansion dates were not related to total early growing season ET ($p > 0.31$ for cumulative ET from January 1 through the end of April, May, or June).

Annual ET showed much less variability than annual P (coefficient of variation (CV) = 4.1% and 17%, respectively; Fig. 3f; Table 2), accounting for 36% (in year 2013) –55% (2012) of annual P. Canopy interception accounted for 163 (standard deviation (SD) = 29) mm y^{-1} of total ET, and was often the predominant component of weekly ET during the dormant season (Fig. 3). ET estimated from P minus Q from two nearby watersheds was 872 mm (SD = 97 mm; Table 3), similar to mean annual tower ET estimates. Cumulative ET estimates from the tower and P minus Q were similar at approximately yearly intervals (Fig. 3g). Hydrologic budget closure did not occur at precisely a 365-day interval due to the time lag between incident P and observed Q resulting from variability in soil water storage (Nippgen et al., 2016).

Overall, cumulative ET (Fig. 3f) showed little interannual variability during spring months, despite differences in leaf expansion. The proportion of ET from the subcanopy (E_S, mm), including the soil surface and small herbaceous vegetation, accounted for 13% of total ET, and was primarily concentrated during the first three months of the year. E_s increased with total ecosystem ET during the early months of the year (Fig. 3c–e). For the first three months of the year, prior to leaf expansion, E_S averaged 37.5 mm (SD = 1.6 mm) among years. Over this time

Table 3
Annual fluxes of water and carbon; precipitation (P), canopy interception (E_I), subcanopy evapotranspiration (E_S), canopy transpiration (E_C), total evapotranspiration (ET), precipitation minus outflow (P–Q), net ecosystem exchange of carbon (NEE), soil CO_2 efflux (F_{soil}) from automated system and transect point measurements, leaf respiration (R_{leaf}), ecosystem respiration (R_E), and gross ecosystem productivity (GEP). E_C is estimated as ET − (E_I + E_S). R_E is estimated as F_{soil} transect + R_{leaf}. GEP is estimated as R_E − NEE.

	2011	2012	2013	2014	2015	Mean (SD)
Water fluxes (mm y^{-1})						
P	1,860	1,639	2,384	1,583	2,094	1,912 (332)
E_I	197	173	243	167	205	197 (30)
E_S	–	–	110	107	115	111 (4)
E_C	506*	621*	517	562	551	551 (45)
ET	813	905	870	836	858	856 (35)
P-Q	1,012	848	790	840	677**	833 (121)
Carbon fluxes (g C m^{-2} y^{-1})						
NEE	−199	−194	−364	−315	−147	−244 (91)
NEE_{sub}	–	–	827	978	1,111	972 (142)
F_{soil} automated	996	975	884	880	939	935 (52)
F_{soil} transect	1,265	1,237	1,117	1,113	1,188	1,184 (68)
R_{leaf}	139	132	121	124	128	129 (7)
R_E	1,404	1,369	1,238	1,237	1,316	1,313 (76)
GEP	1,603	1,563	1,602	1,552	1,463	1,557 (57)

* estimated by subtracting mean E_S when annual E_S was not available.
** Q data only extends through November 2015.

Table 4
Leaf area-based dates of springtime canopy leaf expansion and senescence reaching 25, 50, and 75% of maximum and gross ecosystem productivity (GEP) based dates of growing season start, end, and length.

Leaf area-based growing season metrics	2011	2012	2013	2014	2015
Canopy leaf expansion date					
25%	110	103	119	121	114
50%	114	108	126	125	123
75%	117	113	133	130	131
Canopy leaf senescence date					
75%	289	288	296	296	297
50%	298	294	303	302	301
25%	308	300	310	309	307
Growing season length (days)					
25% range	199	198	192	189	194
50% range	185	187	178	178	179
75% range	173	176	164	167	167

GEP-based growing season metrics	2011	2012	2013	2014	2015
Growing season initiation date	90	95	104	103	93
Growing season termination date	315	312	320	311	311
Growing season length (days)	226	218	217	209	219
Effective growing season length (days)	147	151	145	151	151
Spring midpoint date	126	122	138	129	130
Fall midpoint date	257	263	271	271	270

period, E_S accounted for approximately 71% (SD = 13%) of ET from transpiration and soil evaporation (excluding E_I; Table 3). After leaf expansion, E_S dropped to a fairly consistent 0.14 mm d^{-1} (SD = 0.01) for the majority of the growing season, until fall leaf senescence occurred when it increased slightly to 0.26 mm d^{-1} (SD = 0.09).

Low soil moisture only affected the sensitivity of ET to atmospheric dryness when it occurred late in the growing season. Daily ET increased linearly with mean daily D up to 0.6 kPa, then reached saturation and declined above 0.8 kPa (Fig. 4). Periods of soil moisture limitation, characterized by VWC < 0.3 m^3 m^{-3} (open symbols in Fig. 4), were infrequent through July and did not lead to an apparent decline in the response of ET to D. However, low VWC in August reduced the response of ET to D. The two years that experienced dry August conditions (2011 and 2015) had the second and third earliest leaf senescence, but neither had the earliest. The driest year of our study (2011) reached fall L_{50} later than predicted, based on CDD_{20} (Fig. 2b). A wavelet analysis confirmed that annual variability of ET is well correlated (strong cross-spectra) with environmental variables that show strong seasonality, such as L, temperature, and VWC (Supplementary A.6). Interannual variability in ET was primarily correlated with variability in temperature and VWC, albeit weakly.

3.4. Ecosystem carbon exchange

We observed considerable variability in NEE among years, but variability in NEE was not consistently related to length of the growing season, onset of the growing season, nor growing season end ($p > 0.19$ for all leaf expansion levels in Table 3). The two most productive years, 2013 and 2014, gained an average of 339 g C m^{-2} (Fig. 5, Table 2), but also had two of the shortest growing seasons (Table 3). Compared to the high productivity years, NEE was 40% lower for the years with the longest growing seasons (2011 and 2012), but 45% lower in a year with a comparable growing season length (2015).

Interannual differences in temperature led to large differences in cumulative NEE (Fig. 5f) during the first four months of the year. Dormant season NEE was dominated by F_{soil} (Fig. 5 a–e), and given the exponential response of respiration to temperature (Fig. 6), cumulative annual NEE varied as much as 65 g C m^{-2} among years by DOY 100.

Despite interannual differences in winter respiratory losses, this ecosystem became a cumulative NEE sink (i.e., crossed the zero line) at nearly the same date each year (Fig. 5f). Because winter temperatures directly affect both leaf phenology and respiration, gains in

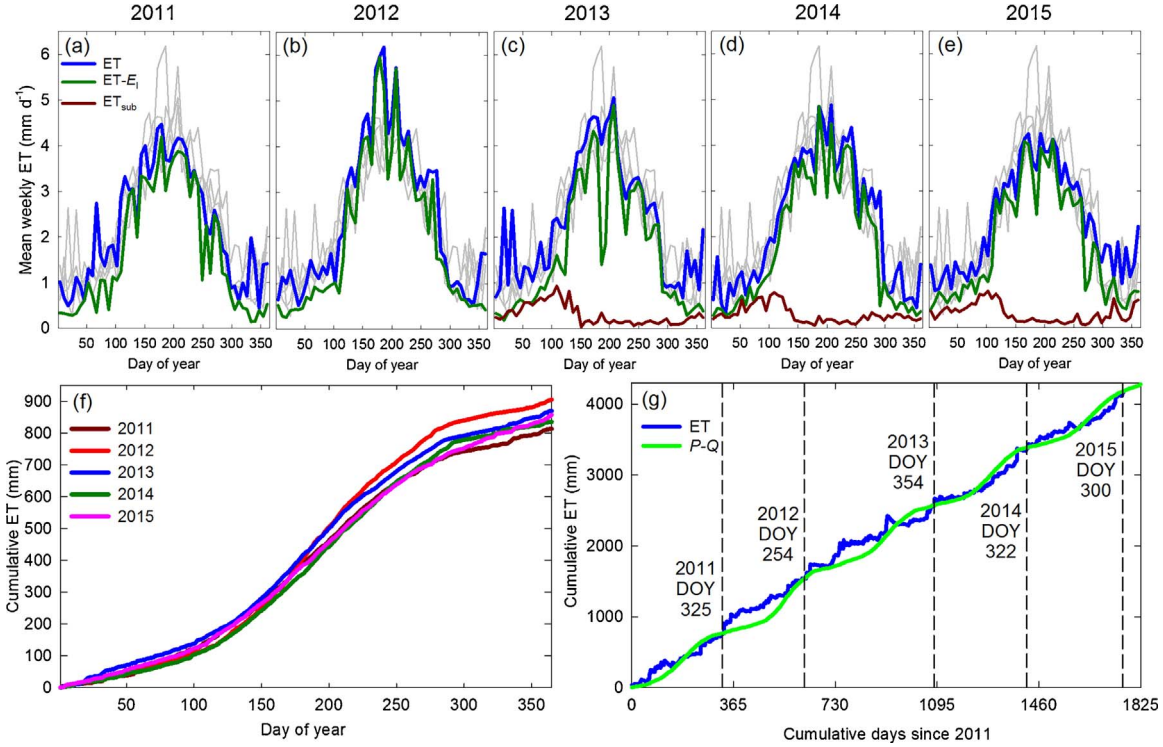

Fig. 3. Time series of (a–e) mean weekly ecosystem evapotranspiration (ET; current year is blue line, other years are gray lines), ET minus evaporation from precipitation intercepted by the canopy (E_I), and subcanopy ET (ET_{sub}) presented as weekly means of daily totals; (f) cumulative ET; (g) total cumulative ET since 2011 and ET estimated as precipitation minus watershed outflow (P–Q); vertical lines represent dates when cumulative ET and P–Q estimates are equal, based on day of current year. (For interpretation of the references to colour in this figure legend, the reader is referred to the web version of this article).

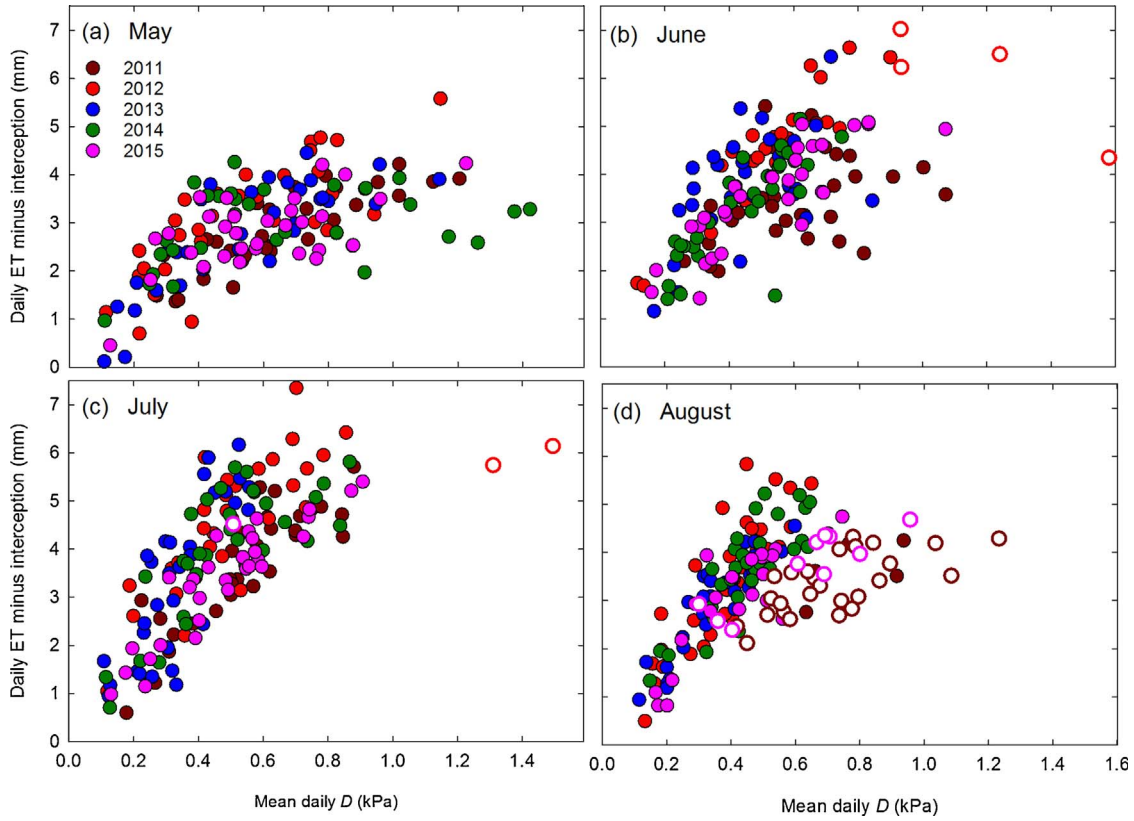

Fig. 4. Daily evapotranspiration (ET) minus evaporation from interception as a function of mean daily vapor pressure deficit (D). Open symbols represent days with volumetric soil water content $< 0.30\ m^3\ m^{-3}$.

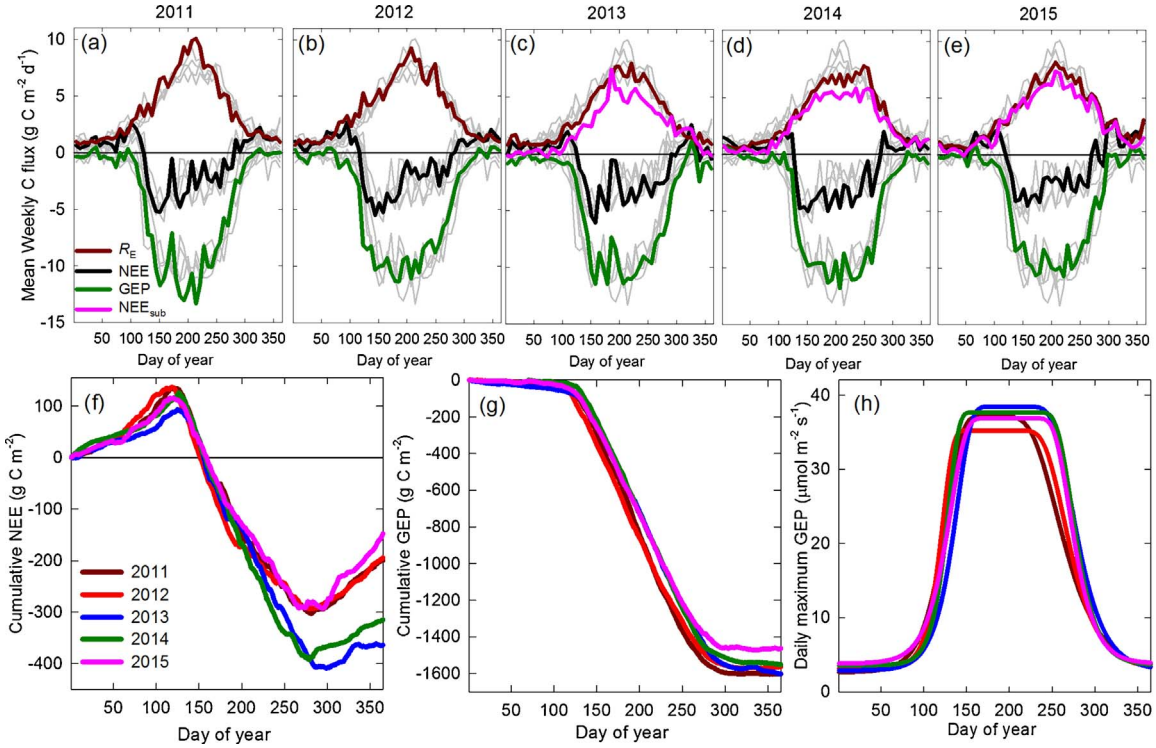

Fig. 5. Carbon fluxes. (a–e) Time series of net ecosystem exchange of carbon (NEE; black lines), ecosystem respiration (R_E; brown lines), gross ecosystem productivity (GEP = NEE – R_E; green lines), and subcanopy NEE (NEE_{sub}; pink lines) presented as weekly means of daily totals (gray lines show data from other years of study); (f) cumulative annual NEE; (g) cumulative annual GEP; (h) estimated potential maximum daily GEP. Negative values represent flux of carbon into the ecosystem, except in (g) where carbon uptake is in positive units. (For interpretation of the references to colour in this figure legend, the reader is referred to the web version of this article).

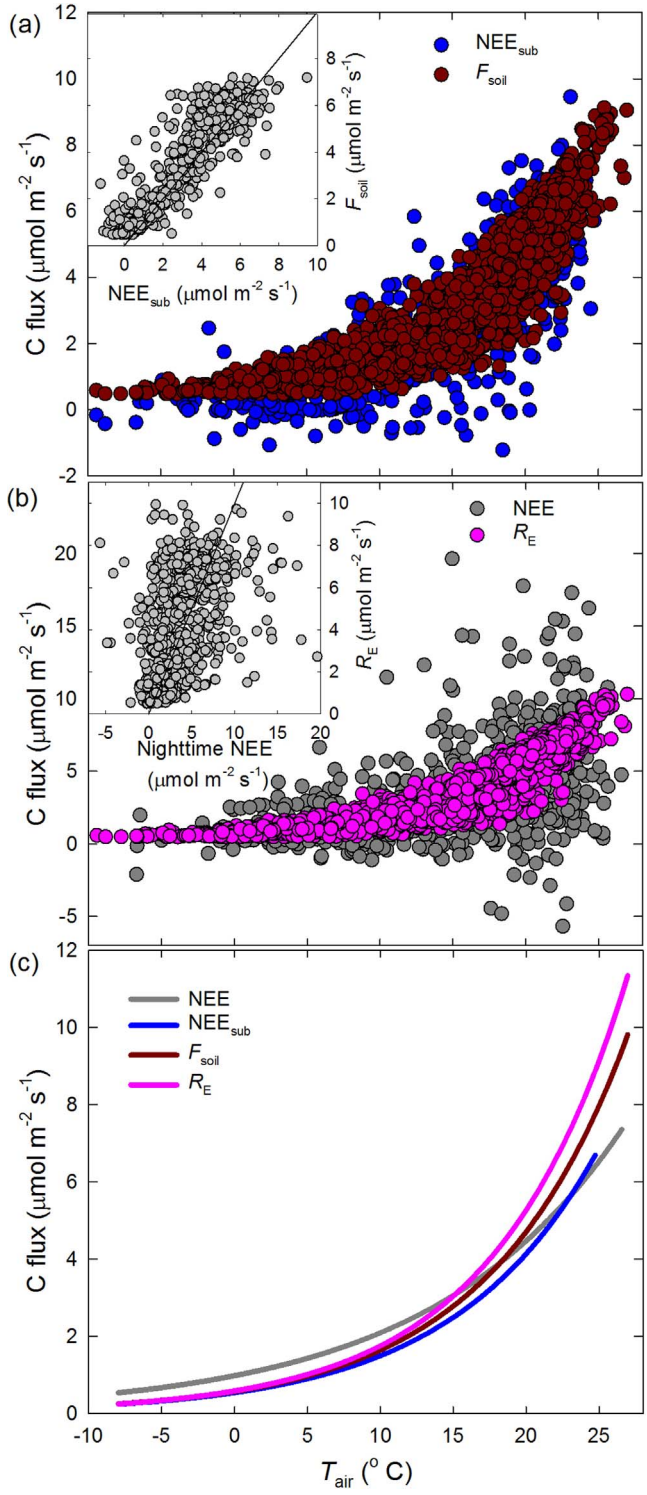

Fig. 6. Components of ecosystem respiration. Daily mean air temperature (T_{air}) versus (a) net ecosystem exchange of carbon from the subcanopy eddy covariance system (NEE$_{sub}$) and soil CO_2 efflux (F_{soil}) estimated from transect measurements, inset shows comparison of daily NEE$_{sub}$ and F_{soil} with 1:1 line; (b) nighttime NEE from the tower eddy covariance system and ecosystem respiration (R_E) estimated as the sum of F_{soil} and leaf respiration, inset shows comparison of nighttime NEE and R_E with 1:1 line; (c) exponential fits to data for data in (a) and (b).

productivity are largely dampened by losses. Thus, despite 2012 having half of its full canopy (L_{50}) 6–18 days earlier than other years, this year switched from a net source to a net sink only 4–7 days earlier.

Leaf expansion dates were weakly correlated with cumulative annual NEE through the end of May (p = 0.058 and 0.073 for dates of L_{25} and L_{50}, respectively), providing some evidence of greater C uptake with earlier leaf expansion. However, by this date each year, the forest remained a net source of C. Expanding this analysis to include cumulative NEE through the end of June, the relationship with leaf expansion dates disappeared ($p > 0.50$).

Differences in annual NEE were driven by mid- to late-growing season conditions. Cumulative NEE for the first several weeks after full leaf expansion (DOY 145–170) showed a strong linear trend during all years (Fig. 5f). The mean uptake over this time (based on absolute slope) ranged from 4.4 to 4.9 g C m^{-2} d^{-1} for all years except for 2015, when sink strength was lower (uptake 3.8 g C m^{-2} d^{-1}). This period of the growing season had the lowest interannual variability in cumulative NEE (SD range from 9.0 to 15.4 g C m^{-2}). After this period, carbon uptake remained fairly consistent during the mild year of 2014. The rainy year of 2013 also showed generally consistent NEE, with a short period of very low uptake from DOY 182 to 196. This period was characterized by 11 consecutive days with rain, totaling 363 mm, and mean daily solar radiation 30% lower than the average of other years. In these two years, late growing season uptake decreased by an average of 34% (DOY 220–260 3.1 and 3.0 g C m^{-2} d^{-1}, respectively). In contrast, in 2011 and 2012, late season uptake decreased by over 50% (2.1 and 1.4 g C m^{-2} d^{-1}, respectively). Year 2015 showed a decline in uptake similar to 2011 and 2012, but since it started with a lower rate of C gain, ended with an uptake of 2.5 g C m^{-2} d^{-1}.

Leaf senescence dates were not correlated with September–November NEE ($p > 0.32$). Although the two years with the earliest dates of leaf senescence were small C sources during this period (loss ~5 g m^{-2}), and the two years with the latest dates were C sinks (uptake ~45 g m^{-2}), the year with the median senescence date was also the largest C source (loss = 19 g m^{-2}).

Cumulative growing season NEE was 15% lower in both 2011 and 2012 than the mild 2014 year (May–Septembers = 426 and 428 vs. 501 g C m^{-2}, respectively; Fig. 5f, Table 3). In comparison, the wet year of 2013 was only 9% lower than 2014 (460 g C m^{-2}), whereas the low NEE during 2014 resulted in the lowest NEE (406 g C m^{-2}). However, since early season respiratory losses led to 2011 and 2012 starting the growing season with an additional 20 g C m^{-2} deficit compared to 2014 (and nearly 50 g compared to 2013), the differences among years were increased. Similar to ET, a wavelet analysis confirmed that interannual variability in NEE was most closely correlated with variability in temperature and VWC rather than L, radiation, or P (Supplementary A.6).

Interannual differences in total NEE appeared to be the result of variability in respiration rather than photosynthesis. Estimated total ecosystem respiration (R_E; excluding stem respiration) was nearly 1240 g C m^{-2} y^{-1} during the two years with the highest NEE (2013 and 2014). Compared to these two years, the warm years of 2011 and 2012 had ~12% higher annual R_E (~150 g C m^{-2} y^{-1}) and 2015 was 6% higher (~75 g C m^{-2} y^{-1}). Our estimates of annual R_E were similar to output from the online flux partitioning tool (five-year mean = 1230 g C m^{-2} y^{-1}). However, during periods with a high frequency of gaps in nighttime data, the online tool output showed large deviations from our estimates, including daily R_E near-zero during the growing season and near the growing season mean during the winter. Nighttime canopy NEE had higher variability and lower temperature sensitivity than F_{soil} (Fig. 6b and c). Estimating R_E using an exponential relationship between T_{air} and nighttime NEE data resulted in mean annual fluxes of 1039 g C m^{-2} (SD = 46), slightly higher than NEE$_{sub}$ and in between our two methods for estimating F_{soil}. However, all approaches followed similar interannual trends. F_{soil} accounted for ~90% of R_E. Among our methods for estimating F_{soil}, transect-based point measurements were 21% higher than measurements from the automated system (Table 2). This difference was due to a combination of higher base respiration at 0 degrees (a-parameter, Eq. (2)) and temperature sensitivity (Q_{10}; Eq. (3)) among the transect measurements (a = 0.533, Q_{10} = 3.935, n = 26) compared to the automated

measurements (a = 0.367, Q_{10} = 3.823, n = 30). However, neither of these parameters was significantly different among methods (p = 0.13 and 0.25, respectively). Transect-based F_{soil} also agreed well with fluxes from the subcanopy eddy covariance system (Fig. 6a and c), suggesting that NEE_{sub} represented primarily respiratory losses. So, although choice of methods may have affected the absolute estimate of F_{soil}, since Q_{10} was similar, the proportionate differences in annual F_{soil} would remain the same. We did not observe any effect of VWC on F_{soil} with either method; however, the measurement periods included only the moderately dry period during fall of 2013. Carbon losses from R_{leaf} occurred only at night when foliage was present, contributing ~10% of annual R_E (Table 2).

Annual gross ecosystem productivity (GEP) in 2011–2014 averaged 1580 g C m^{-2} with low interannual variability (CV = 1.7%; Fig. 5, Table 2). Year 2015 followed a general pattern similar to other years, but with lower average daily GEP during the growing season, resulting in 117 g C m^{-2} lower GEP. Weekly GEP was near zero during the dormant period early in the year, increased rapidly with leaf expansion, and exhibited minor variability during the growing season, before declining back to nearly zero after leaf senescence. Comparing the warmer 2011 and 2012 growing seasons with cooler 2013 and 2014 growing seasons (Fig. 1, Table 2), the warmer years had higher peak R_E, occurring around DOY 200, that coincided with a period of lower NEE (Fig. 5a and b). These factors resulted in consistent linear trends in cumulative growing season GEP (Fig. 5g), nearly parallel among years, as opposed to divergent patterns in cumulative NEE (Fig. 5f). Consistent with earlier leaf expansion, 2012 showed higher cumulative C gain, although not higher daily uptake, throughout most of the growing season. Daily GEP increased with total daily photosynthetically active radiation (PAR) up to approximately 80% of the daily theoretical maximum, at which point GEP leveled-off (data not shown). Daily PAR averaged 71% of the theoretical maximum from May to September (Fig. 1) and was limiting (< 80% of maximum) 56% of growing season days during warmer years (2011, 2012, and 2015) and 70% of days in the milder years (2013 and 2014). Conditions of low PAR occurred on ~2/3 of mornings and ~1/2 of afternoons.

Growing season length based on changes in peak daily GEP (GEP_{max}) ranged as much as 19 days among years (Table 4, Fig. 5h). GEP-derived estimates of the start and end of the growing season did not correspond with dates of L_{25}, L_{50}, or L_{75} ($p > 0.29$); however, dates of spring and fall L_{75} were weakly-correlated with the mid-points of spring and fall GEP_{max} (peak of first derivatives; p = 0.089 and 0.064, respectively). Springtime GEP_{max} was higher in 2012 than other years due to a combination a relatively early initiation of the growing season and rapid development of photosynthetic capacity (although not the top ranked of either of these metrics). Two of the years with the lowest annual NEE (2011 and 2012) also showed earlier declines in fall GEP_{max}, compared to other years.

3.5. Long-term climate trends

Long-term T_{air} trends at our study site have enabled a longer growing season. Based on the relationships between either heating or cooling degree days and dates of L_{50} (Fig. 2), conditions have had no effect on timing of leaf expansion but would enable later leaf senescence, increasing the growing season length by an estimated eight days since 1936 (Fig. 7). Assuming an average daily NEE of 4.6 g C m^{-2}, this increase in growing season length would result in < 2% additional annual NEE per decade), in the absence of changes in NEE due to increases in atmospheric CO_2 over this period. Long-term interannual variability of growing season length was high, with a range of over 30 days (mean = 174 days, SD = 8.8 days). Growing season length was above the long-term mean for only 23 of the past 27 years. Thus, the conditions of our five-year study captured only the upper range of variability in growing season length. Conditions affecting leaf expansion were independent of conditions affecting leaf senescence; no correlation between HDD_0 and CDD_{20} was observed (p = 0.88).

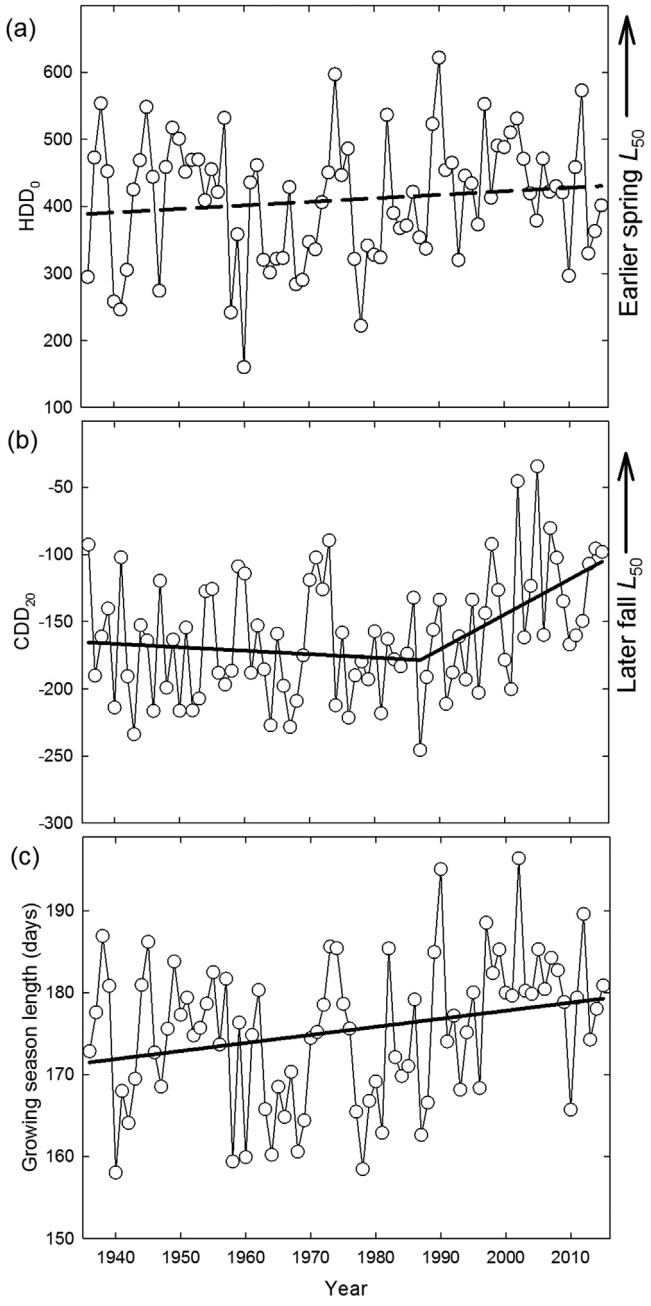

Fig. 7. Temporal trends from long term data at Coweeta Hydrologic Laboratory. (a) heating degree days above 0 °C between day of year 17–83 (HDD_0); slope of linear regression was a non-significant 0.53 HDD_0 y^{-1} (r^2 = 0.01, p = 0.24); (b) cooling degree days below 20 °C between day of year 210–290 (CDD_{20}), piecewise linear regression determined significant breakpoint at year 1987 (r^2 = 0.19, p = 0.0008) with slopes −0.26 and 2.62 CDD_{20} y^{-1} before and after breakpoint, respectively (slope of linear regression 0.57 CDD_{20} y^{-1}; r^2 = 0.08, p = 0.007); (c) growing season length based on estimated dates of canopy leaf area above 50% of maximum (L_{50}), slope of linear regression 0.10 days y^{-1} (r^2 = 0.07, p = 0.016).

Observed long-term temperature trends provide a stronger driver for respiration than growing season length. Increases in long-term T_{air} have resulted from an increased frequency of hot days during the peak of the growing season (Fig. 8a and b). Days with mean T_{air} > 25 °C were infrequent prior to 1995, occurring only 48 times and zero times in 42 out of those 59 years. In contrast, mean daily T_{air} has exceeded 25 °C for at least a week's worth of days in seven of the past 11 years and has exceeded 23 °C for at least 1/3 of the growing season for 13 of

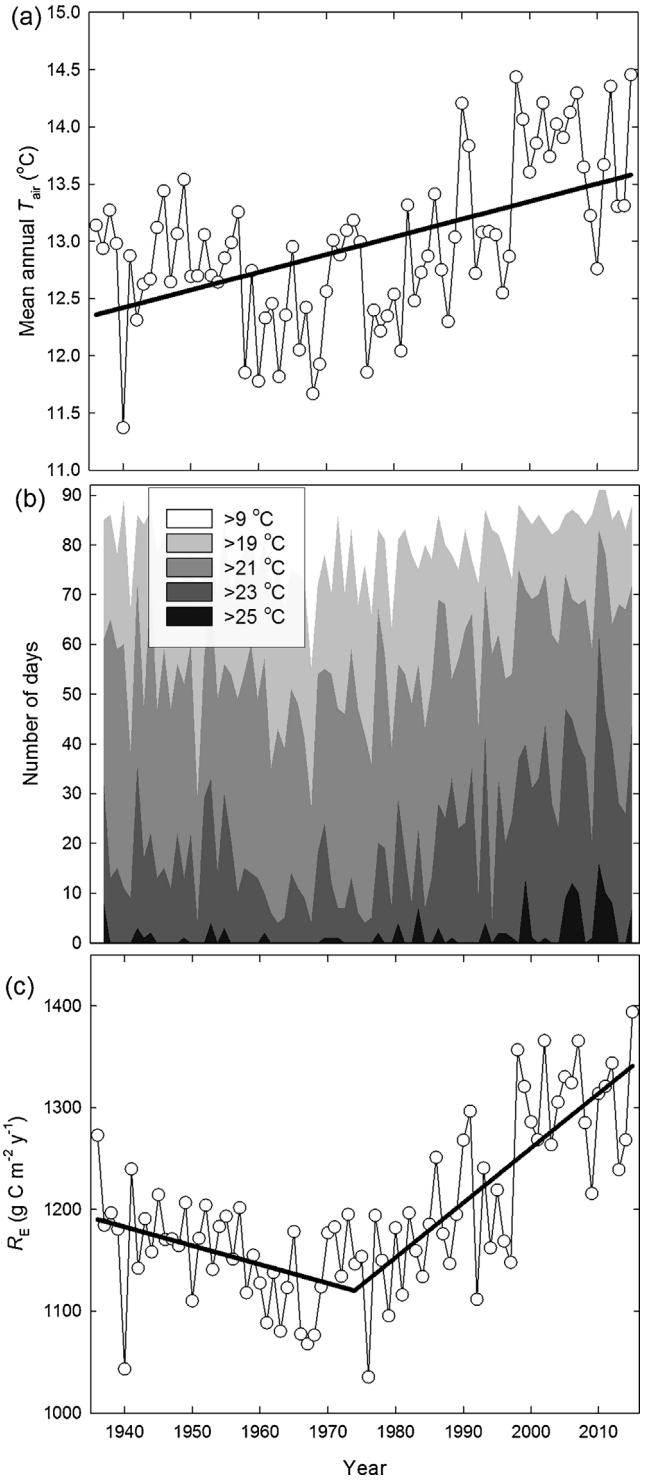

Fig. 8. Temporal trends from long term data at Coweeta Hydrologic Laboratory. (a) mean annual air temperature (T_{air}), slope of regression 0.016 °C y^{-1} ($r^2 = 0.27$, $p < 0.0001$); (b) number of days during the peak of the growing season (June–August) exceeding specified temperatures; (c) estimated long-term ecosystem respiration (R_E), breakpoint of piecewise linear regression at year 1974 ($r^2 = 0.59$, $p < 0.0001$).

the past 18 years. Daily R_E in this ecosystem doubles with each 6.2 °C increase in T_{air} (Fig. 6c), so while an increase in daily T_{air} from 12 to 14 °C would result in an increase in daily R_E of 0.5 g C m^{-2}, an increase from 22 to 24 °C would result in an increase of 1.6 g C m^{-2}. Framed another way, gains in NEE associated with one additional growing season day would be completely offset by R_E if T_{air} increased from 22 to 24 °C on just three days. The increasing frequency of hot days has led to a 20% increase in annual R_E since 1974 (220 g C m^{-2}; Fig. 8c).

4. Discussion

In this study, we examined the direct and indirect effects of temperature on NEE and ET in a mesic, montane, deciduous forest. We expected annual ET to increase with warmer temperatures, due to an extended growing season length and higher *D*. We also expected NEE to either increase or decrease, depending on whether warmer temperatures had a stronger effect on growing season length or respiration. Despite interannual differences in leaf phenology, we found no evidence that growing season length, start date, or end date affected annual ET or NEE in this system. This result is not surprising, as the maximum difference in growing season length among years was nine days (relative to > 200 day growing season length at this site), and three of the five years had similar growing season lengths. Furthermore, we could not separate the interacting effects of growing season length and growing season climate variability making it difficult to detect patterns with only 5 years of data. The most intriguing results emerging from our analysis was that while climatic conditions resulted in large interannual variability in NEE, they produced only minor interannual variability in ET

4.1. Drivers and effects of leaf phenology

The strong temperature dependence of leaf phenology in this system (Fig. 2) and throughout much of the northern hemisphere (Parry et al., 2007), suggests that rising temperatures will lead to an earlier start and later end of the growing season (Fig. 7c). The comparative timing of leaf expansion appeared to follow the timing of leaf senescence (2012, followed by 2011, then all other years at approximately the same time; Fig. 2, Table 4), with greater interannual variability of spring than fall. Such a trend has been observed in the northeastern United States, where for each one-day earlier advance in spring, fall senescence occurs approximately 0.6 days earlier (Keenan and Richardson, 2015). Interestingly, the year 2012 with the warmest early-year T_{air} and very high peak growing season T_{air} (Fig. 1, Table 2) also experienced the coolest fall temperatures (i.e., lowest CDD_{20}, Fig. 2), which was not initially apparent from weekly or monthly averages (Fig. 1; Table 2). This observation highlights the importance of identifying relationships that capture threshold events (e.g., HDD or CDD) in order to predict how short-term (i.e., daily to weekly) climate variability will affect longer-term processes.

Although the start of the growing season was more variable than the end during our five-year study, long-term data suggest that the end of the growing season has been more sensitive to climate change than the beginning (Fig. 7). This result is consistent with a comparable stand at the Morgan-Monroe State Forest (MMSF) in the central United States (Dragoni et al., 2011), though that study reported a dramatic trend of delayed leaf senescence dates (~30 days over a 10-year period) that was not observed in our data. Coweeta is a lower-latitude and warmer site than MMSF, which may have resulted in less sensitive phenological responses to increasing temperatures. Additionally, the complex topography around the Coweeta tower frequently results in cold air drainage at night, particularly during periods of low humidity (Novick et al., 2016b), which may buffer leaf phenology at low elevations against warming trends.

We did see evidence of a seasonal increase in NEE and potential GEP with an earlier spring (Fig. 5). Observed seasonal patterns in *L* generally agreed with patterns in maximum photosynthetic rates (Table 4). However, we note that when comparing phenological metrics from each of these methods, it important to consider the photosynthesis development and recession velocities (slopes in Fig. 5h; Gu et al., 2003) in addition to growing season start and end dates to fully capture the potential for C uptake. For example, in 2012, the growing season initiation day was one week later than 2013, but the rate of increase in

photosynthesis was 19% higher, resulting in higher potential GEP during for most of the 2012 spring (Fig. 5h; Supplementary A.5). The effect of warmer temperatures near the beginning of the growing season had a greater positive effect on photosynthesis than respiration, consistent with broader observed trends (Piao et al., 2008; Richardson et al., 2017), and resulted in a modest C gain during the spring. The warm conditions in January through March of 2012 led to an advance of leaf expansion by approximately two-weeks compared to cooler years (Fig. 2), consistent with remotely sensed estimates in this ecosystem (Hwang et al., 2014) and others across the United States (Wolf et al., 2016). A synthesis of U.S. eddy covariance data showed an average increase in C uptake of 15 g m^{-2} during March–May of 2012, compared to typical years with cooler springs (Wolf et al., 2016). We observed an increased uptake of 34 g C m^{-2} in March–May in 2012 compared to the mean of 2013–2015 and an even more dramatic increase of 63 g C m^{-2} in April–May. However, warm winter temperatures in 2012 resulted in an increase in respiratory losses of 34 g C m^{-2}, reducing the cumulative increase in spring uptake by approximately half.

4.2. Effects of climate on NEE and ET

The increasing frequency of high temperatures in the southern Appalachian region is expected to have a strong influence on C dynamics. Although variability in T_{air} has a linear effect on leaf phenology (Fig. 2), its effect on respiration is exponential (Fig. 6), resulting in a weaker C sink with warmer temperatures (Fig. 5f). Warmer late-winter temperatures at Coweeta led to a greater increase in cumulative photosynthesis through the spring (driven by evergreen carbon uptake and earlier canopy leaf-out), compared to respiration, resulting in a slight enhancement in C gain. In contrast, cool winter temperatures in the mature deciduous forest at MMSF suppressed winter R_E, contributing to enhanced annual C uptake (Dragoni et al., 2011). Warmer summer temperatures at Coweeta, particularly the increasing frequency of very warm days, explained much of the interannual variability in NEE, as well as increased respiratory losses of C over time (Fig. 8). Temperature-sensitivity of soil respiration (i.e., Q_{10}) was higher than most deciduous broadleaf forests (Wei et al., 2010), contributing to lower annual NEE than comparable forests and making C storage in this system particularly vulnerable to warming. Increasing winter T_{air} since the 1980s at Coweeta (Laseter et al., 2012; Ford et al., 2011) has likely muted any long-term gains in C uptake resulting from increasing growing season length.

Unlike temperature, variability in summer precipitation had a negligible effect on NEE and GEP. Across many deciduous broadleaf forests, NEE can be suppressed if precipitation is very low (Wolf et al., 2016) or abnormally high (Fu et al., 2017). Similarly, drought reduced annual GEP by up to 12%, compared to preceding years in a central NC forest (Novick et al., 2015), and GEP declined linearly with increasing soil water deficit in a central United States forest (Brzostek et al., 2014). We observed declines in daily NEE associated with cloudy, rainy days. Solar radiation in the valley around the Coweeta tower is frequently suppressed due to orographic precipitation and morning fog (Novick et al., 2006), likely resulting in lower annual GEP and NEE than other mature broadleaf forests, although not in large interannual variability. Daily PAR was limiting (< 80% of maximum, the point of GEP saturation) approximately 62% of growing season days at Coweeta, compared to only 50% of days at a more productive broadleaf forest in central NC (Novick et al., 2015). Compared to GEP-based growing season metrics from broadleaf forests in Tennessee and Massachusetts, USA (Gu et al. 2003), Coweeta had a higher effective daily maximum photosynthetic rate and longer growing season length (Supplementary A.5), suggesting that high capacity for C uptake was constrained by other environmental factors. Additionally, the topographic position of our study site likely receives downslope subsidies of water (Hawthorne and Miniat 2017), further reducing the frequency of dry soil conditions. Although we did observe seasonal variability in soil moisture among years, climatic conditions at Coweeta did not result in drought conditions during our study period (Figs. 1,4). Even in the absence of drought, annual tree growth of some species at Coweeta has been shown to decline with decreasing numbers of small storms during the growing season (Elliott et al., 2015a, Elliott et al., 2015a, b). In that study, oak species were less sensitive to drought than birch and tulip poplar at low elevations. Therefore, in our mixed species stand, the abundance of oak species (16% of total *L*; Table 1) may help to buffer ecosystem-scale C dynamics against increasing *P* variability. However, given trends toward mesophication of eastern forests (i.e., decline of oak and increasing dominance of red maple and tulip poplar; Nowaki and Abrahms 2008), ecosystem response to changing precipitation patterns should be considered along with response to rising temperatures.

Severe drought conditions may suppress soil respiration (Davidson et al., 1998), the main determinant of ecosystem respiration in this system. Unlike a previous study at this site (Nuckolls et al., 2009), we did not find evidence of soil moisture limitations on F_{soil}. However, the timing of the F_{soil} measurement campaigns did not include the 2011 growing season, the driest part of the larger study period (Fig. 1). Nevertheless, throughout our study, soil moisture was consistently above 0.2 m^3 m^{-3}, the point where soil water limitation occurs in other systems (Ford et al., 2012; Oishi et al., 2013). Thus, the effects of soil water drought on R_E, and subsequently NEE, will likely be secondary to the effects of increasingly high temperatures, and atmospheric drought, at this site (Novick et al., 2016b).

Low interannual variability in ET (Fig. 3) is consistent with other mature, deciduous forests in the southeastern United States. A similar-aged stand in central NC had an eight-year mean ET of 720 mm y^{-1} (SD = 78, CV = 11%), which included moderate and severe droughts (Novick et al., 2015). In that study, interannual variability in ET in the deciduous stand was not related to growing season length, but was correlated with ET from an adjacent evergreen pine plantation, indicating that climate was a stronger driver than phenology on interannual variability in ET. Previous work at that site showed that daily transpiration reached a maximum level at moderate *D* (similar to Fig. 4 in this study) and that high-*D* days typically coincided with drought periods (Oishi et al., 2010). Thus, transpiration on days with high *D* was no higher, and often lower, than on days with moderate *D*. Furthermore, days with low *D* were often associated with rainfall, so the low transpiration was offset by higher amounts of evaporation of precipitation intercepted by the canopy. So although predicted increases in *D* are expected to limit surface conductance across many ecosystems (Novick et al., 2016a), the interannual differences in growing season *D* experienced during this five-year study (Fig. 1) had a negligible effect on annual ET. This may also reflect that, even if high *D* reduces stomatal conductance (which would tend to decrease ET), it also increases the driving force for evaporation (which would tend to increase ET). Thus, consistent with a broader synthesis, predicted changes in precipitation are likely to affect runoff more than ET (Leuzinger and Korner 2010). Indeed, long-term data extending back to the mid-1930s from the three, low-elevation Coweeta watersheds we analyzed in this study (Fig. 3g) showed that precipitation alone explained ~72% of the variability in annual runoff (*Q*) and that precipitation along with potential ET explained ~90% of the variability in *Q* (Caldwell et al., 2016). If this general pattern holds in other areas of the Southern Appalachians and across a wider range of climatic conditions, this consistency in ET suggests that water yield from headwater watersheds in the southern Appalachian biome, serving ten million people living in the southern US (Caldwell et al. 2016), may be particularly sensitivity to future changes in total precipitation.

Conditions of low soil moisture were rare during the peak of the growing season and did not appear to lead to reductions in the sensitivity of ET to *D*. Transpiration estimates from sap flux measurements taken at nearby plots confirm that low-elevation trees can maintain

consistent water use throughout drought (Hawthorne and Miniat 2017). However, relatively dry periods in August of 2011 and 2015 appeared to further restrict ET (Fig. 4). These results suggest that soil moisture only limited ET in these low-elevation cove forests when it occurred at the end of the growing season. Late-growing season drought has been linked to earlier leaf senescence in low-elevation forests at Coweeta, based on remotely-sensed data (Hwang et al., 2014). Based on our data, timing and magnitude of low soil moisture did not appear to affect leaf senescence at the whole canopy scale. However, drought-deciduous species, such as tulip poplar, red maple, and blackgum (Marchin et al., 2010) accounted for over 1/3 of *L* within the eddy covariance tower footprint (Table 1) and may have contributed to seasonal variability in ET, if not a clear signal in the PhenoCam data.

The species composition and structure of southern Appalachian forests has an important influence on carbon and water dynamics. The canopy comprises a mixture of species with a range of xylem anatomies (ring- and diffuse-porous) and hydraulic stress strategies (isohydric and anisohydric). Isohydric, diffuse-porous species such as red maple may show declines in transpiration and productivity when soil water becomes limiting, whereas anisohydric, ring-porous species, namely oaks, may have roots that can access a deeper supply of water and be largely unaffected (Matheny et al., 2017). Thus, species diversity in the canopy is expected to moderate drought effects on NEE and ET, compared to stands dominated by more mesic species (Oishi et al., 2010; Novick et al., 2015). The contribution of understory vegetation has been shown to lead to similar annual transpiration among stands with differing densities (Roberts 1983) and species composition (Kagawa et al., 2009). In our study, prior to leaf expansion, interception of radiation by the canopy is low and ecosystem ET is dominated by evaporation from the soil and transpiration from the evergreen shrub, rhododendron (Fig. 3). Thus, earlier leaf expansion did not correspond to an earlier increase in ET.

Although the structure of the forest overstory typically controls density and water use of understory species (e.g., Kagawa et al., 2009), in the southern Appalachians the increasing coverage of rhododendron may exert a strong influence on canopy NEE and ET in the future (Elliott et al., 2015a, Elliott et al., 2015a, b). However, since the presence of this species also inhibits recruitment of canopy trees (Nilson et al., 2001), the longer-term effect of rhododendron expansion may be reduced ET and reduced aboveground productivity (Bolstad, Elliott, and Miniat, in review).

5. Conclusions

Mature forests in the mesic, southern Appalachian mountain region have a strong potential for C uptake and storage, and regulate surface water supply. Warming in the region has likely extended the growing season, but these changes have been less dramatic than in some comparable forests and appear to have only a minimal effect on water and carbon dynamics. The increasing frequency of warm days is expected to increase respiratory losses, likely reducing the potential for C sequestration, even in the absence of drought. Forest ET shows low interannual variability, meaning that the increasing variability in precipitation will result in greater fluctuations in water yield from these forests. Seasonally, understory ET may compensate for phenology-driven changes in canopy ET. Uncertainty remains about how severe growing season droughts may affect these ecosystem processes.

Acknowledgements

We would like to thank Christine Sobek and Neal Muldoon for experimental setup and field support, Stephanie Laseter and Peter Caldwell for long-term data, Paul Decker and Isabel Hillman for field measurements, Chris Maier and Daniel McInnis for technical support with soil CO_2 efflux equipment, Andrew Richardson, Tom Milliman, and Dave Hollinger for PhenoCam data and support, and Chris Geron, Tom O'Halloran, Donna Schwede, and Paul Stoy for providing helpful comments on earlier versions of this manuscript. We also thank all of the people, past and present who have collected and curated the long-term data record for Coweeta Hydrologic Laboratory.

This research was supported by funding from the USDA Forest Service, Southern Research Station, EPA agreement number 13-IA-11330140-044, USDA NIFA Agriculture and Food Research Initiative Foundational Program (AFRI), award number 2012-67019-19484, National Science Foundation, Long-Term Ecological Research (LTER) program, award #DEB-0823293 and #DEB-1440485. The views expressed in this article are those of the authors and do not necessarily represent the views or policies of the U.S. EPA.

Appendix A. Supplementary data

Supplementary data associated with this article can be found, in the online version, at https://doi.org/10.1016/j.agrformet.2018.01.011.

References

Baldocchi, D., Chu, H., Reichstein, M., 2017. Inter-annual variability of net and gross ecosystem carbon fluxes: a review. Agric. For. Meteorol. 249, 520–533. http://dx.doi.org/10.1016/j.agrformet.2017.05.015.

Ballantyne, A., Smith, W., Andregg, W., Kauppi, P., Sarmiento, J., Tans, P., Shevliakova, E., Pan, Y., Poulter, B., Anav, A., Friedlingstein, P., Houghton, R., Running, S., 2017. Accelerating net terrestrial carbon uptake during the warming hiatus due to reduced respiration. Nat. Clim. Change 7, 148–152.

Bolstad, P.V., Mitchell, K., Vose, J.M., 1999. Foliar temperature-respiration response functions for broad-leaved tree species in the southern Appalachians. Tree Physiol. 19, 871–878.

Brzostek, E.R., Dragoni, D., Schmid, H.P., Rahman, A.F., Sims, D., Wayson, C.A., Johnson, D.J., Phillips, R.P., 2014. Chronic water stress reduces tree growth and the carbon sink of deciduous hardwood forests. Global Change Biol. 20, 2531–2539. http://dx.doi.org/10.1111/gcb.12528.

Burt, T., Miniat, C.F., Laseter, S.H., Swank, W.T., 2017. Changing patterns of daily precipitation totals at the Coweeta Hydrologic Laboratory, North Carolina, USA. Int. J. Climatol. 38, 94–104. http://dx.doi.org/10.1002/joc.S163.

Caldwell, P.V., Miniat, C.F., Elliott, K.J., Swank, W.T., Brantley, S.T., Laseter, S.H., 2016. Declining water yield from forested mountain watersheds in response to climate change and forest mesophication. Global Change Biol. 22, 2997–3012.

Creed, I.F., Spargo, A.T., Jones, J.A., Buttle, J.M., Adams, M.B., Beall, F.D., Booth, E.G., Campbell, J.L., Clow, D., Elder, K., Green, M.B., Grimm, N.B., Miniat, C., Ramlal, P., Saha, A., Sebestyen, S., Spittlehouse, D., Sterling, S., Williams, M.W., Winkler, R., Yao, H., 2014. Changing forest water yields in response to climate warming: results from long-term experimental watershed sites across North America. Global Change Biol. 20, 3191–3208.

Daly, C., Slater, M.E., Roberti, J.A., Laseter, S.H., Swift Jr., L.W., 2017. High-resolution precipitation mapping in a mountainous watershed: ground truth for evaluating uncertainty in a national precipitation dataset. Int. J. Climatol. 37, 124–137. http://dx.doi.org/10.1002/joc.4986.

Davidson, E.A., Belk, E., Boone, R.D., 1998. Soil water content and temperature as independent or confounding factors controlling soil respiration in a temperate mixed hardwood forest. Global Change Biol. 4, 217–227.

Davidson, E.A., Janssens, I.A., 2006. Temperature sensitivity of soil carbon decomposition and feedbacks to climate change. Nature 440, 165–173.

Dragoni, D., Schmid, H.P., Wayson, C.A., Potter, H., Grimmond, C.S.B., Randolph, J.C., 2011. Evidence of increased net ecosystem productivity associated with longer vegetated season in a deciduous forest in south-central Indiana. U. S. A. Global Change Biol. 17, 886–897.

Elliott, K.J., Vose, J.M., Knoepp, J.D., Clinton, B.D., Kloeppel, B.D., 2015a. Functional role of the herbaceous layer in eastern deciduous forest ecosystems. Ecosystems 18, 221–236. http://dx.doi.org/10.1007/s10021-014-9825-x.

Elliott, K.J., Miniat, C.F., Pederson, N., Laseter, S.H., 2015b. Forest tree growth response to hydroclimate variability in the southern Appalachians. Global Change Biol. 21, 4627–4641.

Ford, C.R., Laseter, S.H., Swank, W.T., Vose, J.M., 2011. Can forest management be used to sustain water-based ecosystem services in the face of climate change? Ecol. Appl. 21, 2049–2067.

Ford, C.R., McGee, J., Scandellari, F., Hobbie, E.A., Mitchell, R.J., 2012. Long- and short-term precipitation effects on soil CO_2 efflux and total belowground carbon allocation. Agric. For. Meteorol. 156, 54–64.

Fu, Z., Stoy, P.C., Luo, Y., Chen, J., Sun, J., Montagnani, L., Wohlfahrt, G., Rahman, A.F., Rambal, S., Bernhofer, C., Wang, J., Shirkey, G., Niu, S., 2017. Climate controls over the net carbon uptake period and amplitude of net ecosystem production in temperate and boreal ecosystems. Agric. For. Meteorol. 243, 9–18.

Gu, L., Post, W.M., Baldocchi, D., Black, T.A., Verma, S.B., Vesala, T., Wofsy, S.C., 2003. Phenology of vegetation photosynthesis. In: Schwartz, M.D. (Ed.), Phenology: An Integrative Environmental Science. Springer, Dordrecht, the Netherlands, pp. 467–485. http://dx.doi.org/10.1007/978-94-007-6925-0.

Hawthorne, S., Miniat, C.F., 2017. Topography may mitigate drought effects on

vegetation along a hillslope gradient. Ecohydrology 11 (1), e1825. http://dx.doi.org/10.1002/eco.1825.
Hwang, T., Band, L.E., Miniat, C.F., Song, C., Bolstad, P.V., Vose, J.M., Love, J.P., 2014. Divergent phenological response to hydroclimate variability in forested mountain watersheds. Global Change Biol. 20, 2580–2595.
Kagawa, A., Sack, L., Duarte, K., James, S., 2009. Hawaiian native forest conserves water relative to timber plantation: species and stand traits influence water use. Ecol. Appl. 19, 1429–1443.
Keenan, T.F., Richardson, A.D., 2015. The timing of autumn senescence is affected by the timing of spring phenology: implications for predictive models. Global Change Biol. 21, 2634–2641. http://dx.doi.org/10.1111/gcb.12890.
Laseter, S.H., Ford, C.R., Vose, J.M., Swift Jr., L.W., 2012. Long-Term Temperature and Precipitation Trends at the Coweeta Hydrologic Laboratory 43. Hydrology Research, Otto, North Carolina, USA, pp. 890–901.
Leuzinger, S., Körner, C., 2010. Rainfall distribution is the main driver of runoff under future CO_2-concentration in a temperate deciduous forest. Global Change Biol. 16, 246–254. http://dx.doi.org/10.1111/j.1365-2486.2009.01937.x.
Marchin, R., Zeng, H., Hoffmann, W., 2010. Drought-deciduous behavior reduces nutrient losses from temperate deciduous trees under severe drought. Oecologia 163, 845–854.
Martin, J.G., Kloeppel, B.D., Schaefer, T.L., Kimbler, D.L., McNulty, S.G., 1998. Aboveground biomass and nitrogen allocation of ten deciduous southern Appalachian tree species. Can. J. For. Res. 28, 1648–1659.
Matheny, A.M., Fiorella, R.P., Bohrer, G., Poulsen, C.J., Morin, T.H., Wunderlich, A., Vogel, C.S., Curtis, C.S., 2017. Contrasting strategies of hydraulic control in two codominant temperate tree species. Ecohydrology 10. http://dx.doi.org/10.1002/eco.1815.
McLaughlin, B.C., Ackerly, D., Klos, P.Z., Natali, J., Dawson, T.E., Thompson, S.E., 2017. Hydrologic refugia, plants, and climate change. Global Change Biol. 23, 2941–2961. http://dx.doi.org/10.1111/gcb.13629.
Nilson, E.T., Clinton, B.D., Lei, T.T., Miller, O.K., Semones, S.W., Walker, J.F., 2001. Does *Rhododendron maximum* L. (Ericaceae) reduce the availability of resources above and belowground for canopy tree seedlings? Am. Midl. Nat. 145, 325–343.
Nippgen, F., McGlynn, B.L., Emanuel, R.E., Vose, J.M., 2016. Watershed memory at the coweeta hydrologic laboratory: the effect of past precipitation and storage on hydrologic response. Water Resour. Res. 52, 1673–1695.
Novick, K.A., Oren, R., Stoy, P.C., Siqueira, M.B.S., Katul, G.G., 2009. Nocturnal evapotranspiration in eddy-covariance records from three co-located ecosystems in the Southeastern U.S.: implications for annual fluxes. Agric. For. Meteorol. 149, 1491–1504.
Novick, K.A., Walker, J., Chan, W.S., Schmidt, A., Sobek, C., Vose, J.M., 2013. Eddy covariance measurements with a new fast-response, enclosed-path analyzer: spectral characteristics and cross-system comparisons. Agric. For. Meteorol. 181, 17–32.
Novick, K.A., Brantley, S., Miniat, C.F., Walker, J.T., Vose, J.M., 2014. Inferring the contribution of advection to total ecosystem scalarfluxes over a tall forest in complex terrain. Agric. For. Meteorol. 185, 1–13.
Novick, K.A., Oishi, A.C., Ward, E.J., Siqueira, M.B.S., Juang, J.Y., Stoy, P.C., 2015. On the difference in the net ecosystem exchange of CO_2 between deciduous and evergreen forests in the southeastern United States. Global Change Biol. 21, 827–842.
Novick, K.A., Ficklin, D.L., Stoy, P.C., Williams, C.A., Bohrer, G., Oishi, A.C., Papuga, S.A., Blanken, P.D., Noormets, A., Sulman, B.N., Scott, R.L., Wang, L., Phillips, R.P., 2016a. The increasing importance of atmospheric demand for ecosystem water and carbon fluxes. Nat. Clim. Change 6, 1023–1027.
Novick, K.A., Oishi, A.C., Miniat, C.F., 2016b. Cold air drainage flows subsidize montane valley ecosystem productivity. Global Change Biol. 22, 4014–4027.
Nowaki, G.J., Abrahms, M.D., 2008. The demise of fire and “mesophication” of forests in the eastern United States. Bioscience 58, 123–138.
Nuckolls, A.E., Wurzburger, N., Ford, C.R., Hendrick, R.L., Vose, J.M., Kloeppel, B.D., 2009. Hemlock declines rapidly with hemlock woolly adelgid infestation: impacts on the carbon cycle of southern Appalachian forests. Ecosystems 12, 179–190.
Oishi, A.C., Oren, R., Novick, K.A., Palmroth, S., Katul, G.G., 2010. Interannual invariability of forest evapotranspiration and its consequence to water flow downstream. Ecosystems 13, 421–426.
Oishi, A.C., Palmroth, S., Butnor, J.R., Johnsen, K.H., Oren, R., 2013. Spatial and temporal variability of soil CO_2 efflux in three proximate temperate forest ecosystems. Agric. For. Meteorol. 171–172, 256–269.
Palmroth, S., Maier, C.A., McCarthy, H.R., Oishi, A.C., Kim, H.S., Johnsen, K.H., Katul, G.G., Oren, R., 2005. Contrasting responses to drought of forest floor CO_2 efflux in a loblolly pine plantation and a nearby oak-hickory forest. Global Change Biol. 11, 421–434.
Parry, M.L., Canziani, O.F., Palutikof, J.P., van der Linden, P.J., Hanson, C.E. (Eds.), 2007. Climate Change 2007: Working Group II: Impacts, Adaptation and Vulnerability. Contribution of Working Group II to the Fourth Assessment Report of the Intergovernmental Panel on Climate Change. Cambridge University Press, Cambridge, United Kingdom and New York, NY, USA.
Piao, S., Ciais, P., Friedlingstein, P., Peylin, P., Reichstein, M., Luyssaert, S., Margolis, H., Fang, J., Barr, A., Chen, A., Grelle, A., Hollinger, D.Y., Laurila, T., Lindroth, A., Richardson, A.D., Vesala, T., 2008. Net carbon dioxide losses of northern ecosystems in response to autumn warming. Nature 451, 49–53.
Reichstein, M., Falge, E., Baldocchi, D., et al., 2005. On the separation of net ecosystem exchange into assimilation and ecosystem respiration: review and improved algorithm. Global Change Biol. 11, 1424–1439. http://dx.doi.org/10.1111/j.1365-2486.2005.001002.x.
Richardson, A.D., Black, T.A., Ciais, P., Delbart, N., Friedl, M.A., Gobron, N., Hollinger, D.Y., Kutsch, W.L., Longdoz, B., Luyssaert, S., Migliavacca, M., Montagnani, L., Munger, J.W., Moors, E., Piao, S., Rebmann, C., Reichstein, M., Saigusa, N., Tomelleri, E., Vargas, R., Varlagin, A., 2010. Influence of spring and autumn phenological transitions on forest ecosystem productivity. Philos. Trans. R. Soc. Lond. Ser. B 365, 3227–3246.
Richardson, A.D., Keenan, T.F., Migliavacca, M., Ryu, Y., Sonnentag, O., Toomey, M., 2013. Climate change, phenology, and phenological controls on vegetation feedbacks to the climate system. Agric. For. Meteorol. 169, 156–173.
Richardson, A.D., Hufkens, K., Milliman, T., Aubrecht, D.M., Chen, M., Gray, J.M., Johnston, M.R., Keenan, T.F., Klosterman, S.T., Kosmala, M., Melaas, E.K., Friedl, M.A., Frolking, S., Abraha, M., Alber, M., Apple, M., Law, B.E., Black, T.A., Blanken, P., Browning, D., Bret-Harte, S., Brunsell, N., Burns, S.P., Cremonese, E., Desai, A.R., Dunn, A.K., Eissenstat, D.M., Euskirchen, E., Flanagan, L.B., Forsythe, B., Gallagher, J., Gu, L., Hollinger, D.Y., Jones, J.W., King, J., Langvall, O., McCaughey, J.H., McHale, P.J., Meyer, G.A., Mitchell, M.J., Migliavacca, M., Nesic, Z., Noormets, A., Novick, K., O’Connell, J., Oishi, A.C., Oswald, W.W., Perkins, T.D., Phillips, R.P., Schwartz, M.D., Scott, R.L., Sonnentag, O., Thom, J.E., 2017. PhenoCam Dataset v1.0: Vegetation Phenology from Digital Camera Imagery, 2000–2015. ORNL DAAC, Oak Ridge, Tennessee, USA. http://doi.org/10.3334/ORNLDAAC/1511.
Roberts, J., 1983. Forest transpiration: a conservative hydrological process? J. Hydrol. 66, 133–141.
Sonnentag, O., Hufkens, K., Teshera-Sterne, C., Young, A.M., Friedl, M., Braswell, B.H., Milliman, T., O’Keefe, J., Richardson, A.D., 2012. Digital repeat photography for phenological research in forest ecosystems. Agric. For. Meteorol. 152, 159–177. http://dx.doi.org/10.1016/j.agrformet.2011.09.009.
Wei, W., Weile, C., Shaopeng, W., 2010. Forest soil respiration and its heterotrophic and autotrophic components: global patterns and responses to temperature and precipitation. Soil Biol. Biochem. 42, 1237–1244.
Williams, A.P., Allen, C.D., Macalady, A.K., Griffin, D., Woodhouse, C.A., Meko, D.M., Swetnam, T.W., Rauscher, S.A., Seager, R., Grissino-Mayer, H.D., Dean, J.S., Cook, E.R., Gangodagamage, C., Cai, M., McDowell, N.G., 2013. Temperature as a potent driver of regional forest drought stress and tree mortality. Nat. Clim. Change 3, 292–297.
Wolf, S., Keenan, T.F., Fisher, J.B., Baldocchi, D.D., Desai, A.R., Richardson, A.D., Scott, R.L., Law, B.E., Litvak, M.E., Brunsell, N.A., Peters, W., van der Laan-Luijkx, I.T., 2016. Warm spring reduced carbon impact of the 2012 US summer drought. Proc. Nat. Acad. Sci. U.S.A. 113, 5880–5885.
Zhou, S., Medlyn, B., Sabaté, S., Sperlich, D., Prentice, C., 2014. Short-term water stress impacts on stomatal, mesophyll and biochemical limitations to photosynthesis differ consistently among tree species from contrasting climates. Tree Physiol. 34, 1035–1046.